Science of the Total Environment 640–641 (2018) 543–554

Contents lists available at ScienceDirect

Science of the Total Environment

journal homepage: www.elsevier.com/locate/scitotenv

Future precipitation changes over China under 1.5 °C and 2.0 °C global warming targets by using CORDEX regional climate models

Huixin Li [a,c], Huopo Chen [a,b,*], Huijun Wang [a,b], Entao Yu [a,b]

[a] Nansen-Zhu International Research Centre, Institute of Atmospheric Physics, Chinese Academy of Sciences, Beijing, China
[b] Collaborative Innovation Center on Forecast and Evaluation of Meteorological Disasters, Nanjing University of Information Science and Technology, Nanjing, China
[c] University of Chinese Academy of Sciences, Beijing, China

HIGHLIGHTS

- RCMs can reproduce the characteristics of precipitation extremes over China.
- China will suffer from increased severe precipitation extreme events at 1.5 °C and 2.0 °C warming levels in the future.
- The occurring risks of precipitation extremes will obviously increase across China due to an additional 0.5 °C warming.
- Future changes in atmospheric circulations might account for the increased precipitation extremes across China.

GRAPHICAL ABSTRACT

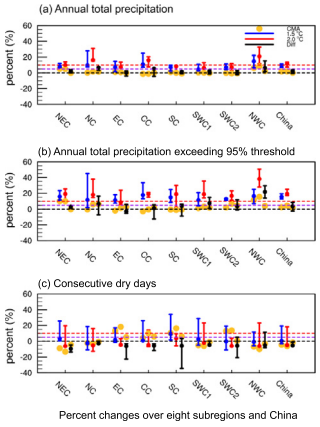

ARTICLE INFO

Article history:
Received 20 March 2018
Received in revised form 25 May 2018
Accepted 25 May 2018
Available online 1 June 2018

Editor: Jay Gan

Keywords:
CORDEX
Precipitation extremes
1.5 °C warming
2.0 °C warming
Risk
China

ABSTRACT

This study aims to characterize future changes in precipitation extremes over China based on regional climate models (RCMs) participating in the Coordinated Regional Climate Downscaling Experiment (CORDEX)-East Asia project. The results of five RCMs involved in CORDEX-East Asia project that driven by HadGEM2-AO are compared with the simulation of CMA-RegCM driven by BCC-CSM1.1. Eleven precipitation extreme indices that developed by the Expert Team on Climate Change Detection and Indices are employed to evaluate precipitation extreme changes over China. Generally, RCMs can reproduce their spatiotemporal characteristics over China in comparison with observations. For future climate projections, RCMs indicate that both the occurrence and intensity of precipitation extremes in most regions of China will increase when the global temperature increases by 1.5/2.0 °C. The yearly maximum five-day precipitation (RX5D) averaged over China is reported to increase by 4.4% via the CMA-RegCM under the 1.5 °C warming in comparison with the baseline period (1986–2005); however, a relatively large increase of 11.1% is reported by the multi-model ensemble median (MME) when using the other five models. Furthermore, the reoccurring risks of precipitation extremes over most regions of China will further increase due to the additional 0.5 °C warming. For example, RX5D will further increase by approximately 8.9% over NWC, 3.8% over NC, 2.3% over SC, and approximately 1.0% over China. Extremes, such as the historical 20-year return period event of yearly maximum one-day precipitation (RX1D) and RX5D, will become more frequent, with occurrences happening once every 8.8 years (RX1D) and 11.5 years (RX5D) under the 1.5 °C warming target, and there will be two fewer years due to the additional 0.5 °C warming. In addition, the intensity

* Corresponding author at: Nansen-Zhu International Research Centre (NZC), Institute of Atmospheric Physics, Chinese Academy of Sciences, PO Box 9804, Beijing 100029, China.
E-mail address: chenhuopo@mail.iap.ac.cn (H. Chen).

https://doi.org/10.1016/j.scitotenv.2018.05.324

of these events will increase by approximately 9.2% (8.5%) under the 1.5 °C warming target and 12.6% (11.0%) under the 2.0 °C warming target for RX1D (RX5D).

1. Introduction

During the last century, global warming has been evident worldwide, with an average surface air temperature increase of 0.85 °C (0.65 °C to 1.06 °C) from 1880 to 2012 (IPCC, 2013). Accompanied by this increase in temperature, there was an obvious increase in climate extremes around the world (WMO, 2010; Piras et al., 2016; Aslam et al., 2017). To avoid suffering from more severe climate extremes, the Paris Climate Agreement proposed a goal to limit global mean surface warming below 2.0 °C and pursue a target of 1.5 °C when compared with preindustrial levels (UNFCCC, 2015).

China comprises about one-fifth of the world's population, with a vast territory and complex topography. Generally, precipitation extremes often result in high impacts on society, the economy, and natural ecosystems in China (Cheng et al., 2014; Liu et al., 2017a; Ye et al., 2018); thus, it is quite necessary to understand the changes in precipitation extremes to mitigate their effects. In recent decades, precipitation extremes and their associated disastrous floods have increased across China (Zhai et al., 2005; Chen et al., 2012a; Wang et al., 2012; Sun and Ao, 2013; Liu et al., 2015), and anthropogenic activities might partially account for this increase (Chen and Sun, 2017; Li et al., 2017). Given that changes in precipitation extremes might link to global warming, the question then arises as to how precipitation extremes will change in the future. Recently, many studies have documented future climate changes across China using global climate model (GCM) simulations. Results suggested that there would be more high-impact precipitation extreme events as well as increased hot days in the future across China (Chen, 2013; Chen et al., 2013; Chen and Sun, 2014; Wang and Chen, 2014; Li et al., 2015; Tian et al., 2015; Xu et al., 2015a; Chen et al., 2017; Liu et al., 2017b).

In comparison with the GCM simulations, Giorgi and Gao (2018) indicated that the regional climate model (RCM) is another effective tool to investigate the changes in precipitation extremes across China. However, there are few concerns regarding this aspect in China using RCMs so far, because of its high computational resource. Recently, the project of Coordinated Regional Climate Downscaling Experiment (CORDEX) that led by the World Climate Research Programme has released the high quality control downscaled climatic datasets on the regional scales, including historical and future simulations (Giorgi et al., 2012). Prior to current research, the RCM performance in simulating the variations of the climate extremes over East Asia has been evaluated and these models generally present relatively higher performance than the GCMs (Ozturk et al., 2012; Oh et al., 2013; Oh et al., 2014; Jin et al., 2015; Kim et al., 2016; Park et al., 2016). Thus, these RCM simulations will be used here to investigate future changes of precipitation extremes across China under different warming targets.

Recently, climate change response to different warming targets (1.5 °C/2.0 °C) have been explored across the world (Karmalkar and Bradley, 2017; King et al., 2017; Huang et al., 2017; Tian et al., 2017; Wang et al., 2017; Zhou et al., 2018) as well as across China (Guo et al., 2016; Xu et al., 2017; Chen and Sun, 2018). However, the analyses of most previous studies just based on the simulations from the GCMs, while fewer concerns can be seen using the RCM simulations. That is, to what extent that climate extremes can be avoided if global temperatures increase by 1.5 °C compared to 2.0 °C will be addressed based on RCMs in this study.

Consequently, the purpose of this study is to conduct comprehensive analyses of future changes in precipitation extremes over China under 1.5/2.0 °C warming targets based on the CORDEX-East Asia project, which will further improve our understanding on climate changes. Accordingly, the structure of this paper is as follows. Section 2 describes the datasets and methods used in this study. Section 3 evaluates the performance of the CORDEX-East Asia project in simulating precipitation extremes over China and further compares the changes of precipitation extremes and atmospheric circulations across China under the 1.5/2.0 °C warming targets. A brief discussion and conclusion finally presented in Section 4.

2. Data and methods

2.1. Datasets

An observational gridded daily precipitation dataset from 1961 to 2014 is used in this study (hereafter referred to as CN05.1). This dataset was developed by Wu and Gao (2013) using an anomaly approach to interpolate 2416 stations across China, with a high horizontal resolution of 0.5° longitude by 0.5° latitude. More detailed information concerning the data construction can be found in Xu et al. (2009) and Wu and Gao (2013).

Six regional climate models that included in the CORDEX-East Asia project are also employed in this study. Five of them were developed in Korea (http://cordex-ea.climate.go.kr/cordex/download.do), including three nonhydrostatic RCMs (HadGEM3-RA, SNU-MM5, and YSU-RSM) and two hydrostatic RCMs (KNU-RegCM and SNU-WRF). Here, HadGEM3-RA (Davies et al., 2005) was developed by the National Institute of Meteorological Research in Korea; KNU-RegCM (Giorgi et al., 2012) was developed by Kongju National University, SNU-MM5 (Cha and Lee, 2014) and SNU-WRF (Skamarock et al., 2005) were developed by Seoul National University, and YSU-RSM (Hong et al., 2013) was developed by Yonsei University. These five RCMs have a horizontal resolution of 50 km (0.44° for HadGEM3-RA), and they are driven by boundary and initial conditions from the historical simulation of HadGEM2-AO. Another RCM simulation (CMA-RegCM) from China is also used here for comparison. The horizontal resolution of the CMA model is 25 km, and its simulation is driven by the initial and boundary conditions from the BCC-CSM1.1 model, which was developed by the National Climate Center in China (Giorgi et al., 2012; Gao et al., 2016). The CMA model provides a daily precipitation output over East Asia, which includes a historical run from 1961 to 2005 and future runs from 2006 to 2099.

The variables employed in this study are daily precipitation, monthly meridional and zonal winds, monthly convective precipitation, monthly sea level pressure, monthly specific humidity, and monthly geopotential height. These RCMs have different time length for both the historical and future simulations. However, the historical run from 1980 to 2005 and the future runs from 2006 to 2049 (except for SNU-MM5 under the RCP8.5 scenario) are available in all of the RCMs. Detailed information concerning the vertical levels, dynamic framework, convective scheme, land surface, and the planetary boundary layer is listed in Table S1. To reduce uncertainties from inter-model differences (Kim et al., 2014), we also calculate the multi-model ensemble median (MME) of the five RCMs that are driven by HadGEM2-AO. For convenience, all of the simulations are bi-linearly interpolated onto 0.5° × 0.5° grids (similar to CN05.1). In addition to the RCMs, the monthly temperature datasets that derived from HadGEM2-AO and BCC-CSM1.1 are also used in this study.

2.2. Methods

A large bias can be generally found in the model simulations when compared with the observations. Thus, a bias correction method

(Sperna Weiland et al., 2010) is first implemented on the basis of the observations.

$$P_{corrected\_\mathrm{mod}} = P_{\mathrm{mod}} \frac{\overline{P}_{CN05}}{\overline{P}_{\mathrm{mod}}} \quad (1)$$

Here, P_{mod} represents the original daily precipitation output for a particular RCM, $\overline{P}_{CN05}$ represents the 20-year average daily precipitation from 1986 to 2005 for CN05.1, $\overline{P}_{\mathrm{mod}}$ represents the 20-year average daily precipitation from 1986 to 2005 for the corresponding RCM, and $P_{corrected\_\mathrm{mod}}$ represents the bias-corrected daily precipitation.

Based on the bias-corrected daily precipitation datasets, we select eleven precipitation extreme indices from the Expert Team on Climate Change Detection and Indices (ETCCDI) to evaluate the changes in precipitation extremes over China. The ETCCDI provides a robust and direct analysis of climate extremes, and some of them have been widely used in China (Chen et al., 2012a; Wang et al., 2012; Chen and Sun, 2015; Dong et al., 2015; Zhou et al., 2015; Wu et al., 2016). The definitions of these precipitation extreme indices can be found in Chen and Sun (2015) or Table S2.

To evaluate the performance of the RCMs in simulating precipitation extremes over China, two metrics (the model performance index (MPI; see Eq. (2)) and the model variability index (MVI; see Eq. (3))) are employed to judge the model performances.

$$MPI_{mf} = \frac{E_{mf} - \overline{E}_f}{\overline{E}_f} \quad (2)$$

$$MVI_m = \sum_{f=1}^{F} \left[\beta_{mf} - \frac{1}{\beta_{mf}} \right]^2 \quad (3)$$

Here, E_{mf} represents the model simulated root mean square (RMS) difference for a given model (m), and a given extreme precipitation index (f). $\overline{E}_f$ represents the median value of the RMS calculation for a given extreme precipitation index (f). F represents the total number of extreme precipitation indices ($F = 11$ in this study), and ${\beta_{mf}}^2$ represents the ratio of the simulated variance compared to the observed variance. A negative value of the MPI generally suggests a relatively higher climate performance than the typical model, and a smaller value of the MVI indicates the relatively better performance of variability for the model (Gleckler et al., 2008).

We use the generalized extreme value (GEV) fitting method to describe the probability and recurrence of extreme precipitation events over China. The annual maximum one-day precipitation (RX1D) and the annual maximum five-day consecutive precipitation (RX5D) are fitted with the GEV distribution. The cumulative density function of the GEV distribution in Eq. (4) has three variables, including the location (ξ), scale (β), and shape (κ) parameters (Wilks, 2011), which are estimated by the maximum likelihood method (Martins and Stedinger, 2000).

$$\begin{aligned} F(x) &= \exp\left\{ -\left[1 + \frac{x-\xi}{\beta} \right]^{-\frac{1}{\kappa}} \right\}, \kappa \neq 0, 1 + \frac{\kappa(x-\xi)}{\beta} > 0 \\ F(x) &= \exp\left\{ -\exp\left[-\frac{x-\xi}{\beta} \right] \right\}, \kappa = 0 \end{aligned} \quad (4)$$

The climate in China is quite complex and it generally varies from regions (Qian and Lin, 2005). To address the changes in precipitation extremes clearly, we separated China into eight sub-regions (Xu et al., 2015b), including Northwestern China (NWC; 36–46°N, 75–111°E), Southwestern China (SWC1: 27–36°N, 77–106°E; SWC2: 22–27°N, 98–106°E), North China (NC; 36–46°N, 111–119°E), Northeastern China (NEC; 39–54°N, 119–134°E), Central China (CC; 27–36°N, 106–116°E), Eastern China (EC; 27–36°N, 116–122°E), and Southern China (SC; 20–27°N, 106–120°E) (Fig. 4).

3. Results

3.1. RCM performance in simulating precipitation extremes over China

Before evaluating the future changes in precipitation extremes over China, we first evaluate the model capability in simulating the precipitation extremes across China. Fig. 1 shows the observed and simulated spatial distributions of the annual total amount of extreme precipitation events (R99p) over China from 1986 to 2005, and Fig. S1 shows the results of heavy precipitation days (R20mm). Both individual RCMs and the MME can well capture the southeast-northwest gradient of precipitation extremes over China. For example, the spatial correlation between the observations and MME is 0.98 (0.98) for R99p (R20mm). Similarly, the southeast-northwest gradient of the total wet-day precipitation (PRCPTOT), the amount of yearly very wet precipitation (R95p), RX5D, RX1D, heavy precipitation days (R10mm), and simple daily precipitation intensity (SDII) are also well reproduced by the individual RCMs, with high spatial correlations of 1.0, 0.99, 0.97, 0.96, 0.99, and 0.97 between the observations and MME, respectively. The consecutive dry days (CDD) presents a different pattern with an obvious northwest-southeast gradient in China (figure not shown), and the spatial correlation between the observations and MME is 0.82. In terms of consecutive wet days (CWD) and precipitation days (R1mm), all RCMs resemble the observed south-north spatial contrast over China (figure not shown), with spatial correlations of 0.78 and 0.97, respectively, between the observations and MME.

Fig. 2 presents a concise statistical analysis of the model performances in simulating eleven extreme precipitation indices over China. Generally, all of the RCMs present good spatial correlations with the observation for most of the indices but with relatively lower spatial correlations for CDD and CWD that range from 0.5 to 0.9 (Fig. 2(d)). It is clear that HadGEM3 is the best model for simulating the spatial patterns of precipitation extremes (Fig. 2(a)–(d)). For example, the lowest (highest) spatial correlation between HadGEM3 and the observations is 0.71 (0.98) for CWD (R95p) among the eleven indices (except for PRCPTOT because the correlations between CN05.1 and all of the RCMs are 1.0 because of the bias-correction processes). In addition, the spatial correlations between CMA (KNU and SNU-MM5) and the observations of PRCPTOT, R10mm, R95p, R99p, RX1D, RX5D, and SDII are all greater than 0.90. The model spreads for R95p, R99p, R1mm, R10mm, and R20mm are relatively small among the eleven indices, with high spatial correlations ranging from 0.9 to 0.99 and relatively low RMS errors (Fig. 2(b), (c)). Overall, the spatial correlations between the MME and observations are greater than 0.78, with RMS errors smaller than 0.75 for all of the indices. Therefore, the MME outperforms the individual RCMs in simulating climatological precipitation extremes over China.

Table 1 summarizes the climatological mean of precipitation extremes during the historical period (1986–2005). Clearly, most of the indices are well reproduced by the RCMs, and the performances of the RCMs are different when simulating the individual indices. For example, HadGEM3 is the best at simulating PRCPTOT, R10mm, R99p, and SDII; SNU-WRF is the best at simulating CDD, CWD, R1mm, R20mm, and R95p; and KNU is the best at simulating RX1D and RX5D.

Fig. 3 further presents the spatially averaged temporal series of RX5D, R95p, and R20mm from 1961 to 2100. Clearly, the MME is the best at simulating variations in precipitation extremes over China from 1986 to 2005. In terms of the observational linear trends of precipitation extremes from 1986 to 2005, we witness weak decreasing trends for CDD (−3.3%/10 yr), SDII (−0.1%/10 yr), and R10mm (−0.6%/10 yr), accompanied with weak increasing trends for CWD (2.6%/10 yr), PRCPTOT (0.6%/10 yr), R1mm (0.8%/10 yr), R20mm (0.0%/10 yr), R95p (0.2%/10 yr), R99p (2.1%/10 yr), RX1D (0.4%/10 yr), and RX5D (1.7%/

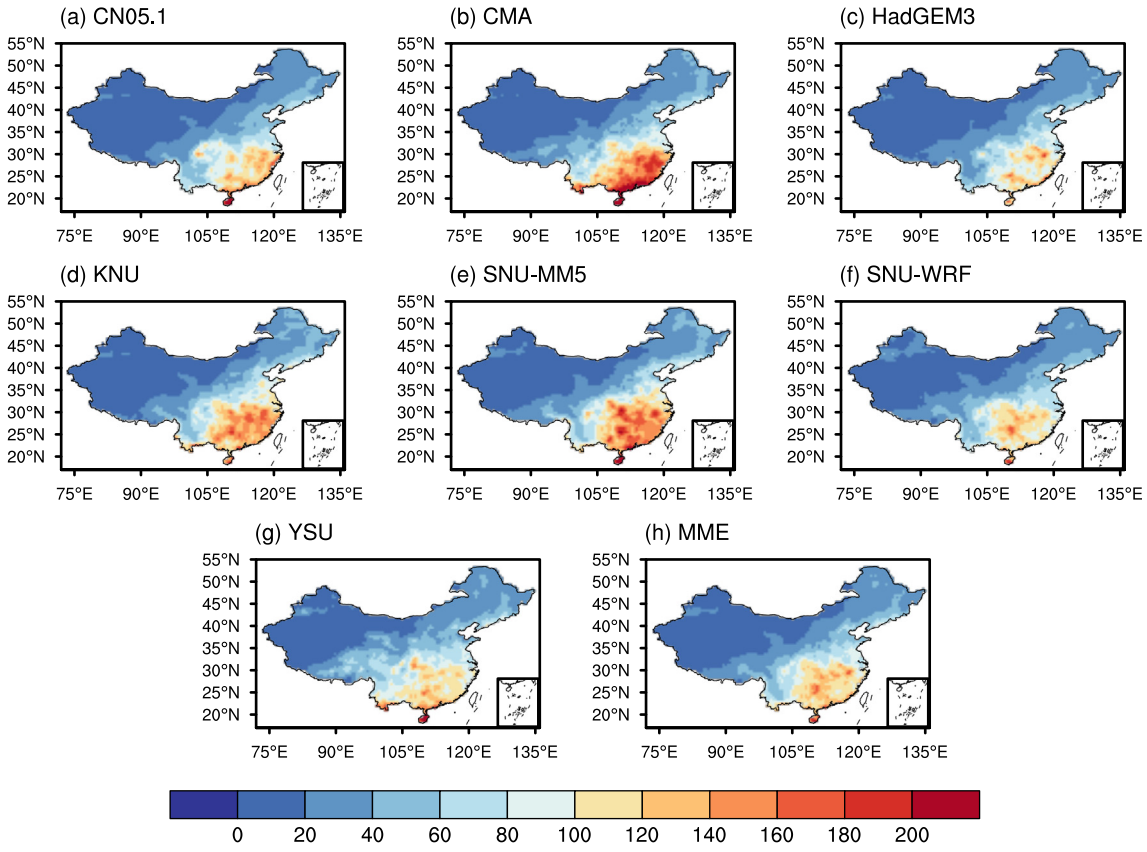

Fig. 1. Climatological distribution of annual total precipitation extremes exceeding the 99% threshold for wet day precipitation (R99p; units: mm) from 1986 to 2005 based on (a) CN05.1, (b) CMA, (c) HadGEM3, (d) KNU, (e) SNU-MM5, (f) SNU-WRF, (g) YSU, and (h) the multimodel ensemble median (MME) of (c)–(g).

10 yr). However, none of these trends is significant at the 95% confidence level based on the Mann-Kendall nonparametric test. This is also the case for most of the individual RCMs.

Then, the additional model performances in simulating the climatological means or interannual variabilities of precipitation extremes over China are further analyzed (Fig. S2). Generally, the model performances of the individual RCMs vary among different extreme precipitation indices. For example, KNU and HadGEM3 are the best two RCMs when simulating climatological means (Fig. S2(a)), while HadGEM3 and CMA are the best two RCMs when simulating interannual variability (Fig. S2(b)). Generally, the MME outperforms most of the individual RCMs when simulating precipitation extremes over China both for the climatological mean and for the interannual variability.

3.2. Changes in precipitation extremes with additional 0.5 °C warming

The above analyses have verified good performances of the CORDEX-East Asia project in simulating precipitation extremes over China. Furthermore, these precipitation extremes will become more frequent or intensified over China in the future (see Fig. 3). Here, we attempt to evaluate the future changes in precipitation extremes when global warming reaches the 1.5/2.0 °C targets. Since the RCMs do not provide global datasets, we use the outputs from the GCMs, which initiate the RCM runs, to calculate the timing of global temperature reaching the warming targets. According to Huang et al. (2017), we define 1.5 °C (2.0 °C) warming as the 11-year smoothed surface air temperature (SAT) that increases by 1.5 °C (2.0 °C) with respect to the period 1861–1900. For BCC-CSM1.1, the SAT will increase by 1.5 °C (2.0 °C) from approximately 2017–2027 (2039–2049) via the RCP4.5 and approximately 2016–2026 (2032–2042) via the RCP8.5. For HadGEM2-AO, the timing of the 1.5 °C (2.0 °C) warming will be from 2022 to 2032 (2040–2050) via the RCP4.5 and 2030–2040 (2039–2049) via the RCP8.5.

Fig. 4 shows the spatial distribution of percent changes in RX5D under different warming targets based on the RCP8.5 scenario, and the results based on the RCP4.5 scenario are similar (figures not shown). Since the timing of 2.0 °C warming under the RCP8.5 scenario is not included in the temporal coverage of the SNU-MM5, we eliminate SNU-MM5 in this case. Generally, the national mean of RX5D is reported to increase by 4.4% via the CMA and 11.1% (9.3% to 13.4%) via the MME of the remaining RCMs (model spread) under the 1.5 °C warming target. For the 2.0 °C warming target, the national mean of RX5D will increase by 5.4% via the CMA and 12.1% (6.0% to 13.5%) via the MME of the remaining RCMs (model spread). However, large differences can be observed over different regions. When the temperature increases by 1.5 °C, RX5D increases over NWC, NC, NEC, EC, SC, and CC, but large discrepancies occur among RCMs over SWC1. When the temperature increases by 2.0 °C, all of the RCMs project that RX5D increases significantly over NEC, NC, and NWC (significant at the 90% confidence level). Besides, most of the RCMs also project an increase of RX5D over CC, SC, and EC. Due to the additional 0.5 °C warming, the magnitude of RX5D based on the MME will be further strengthened over NWC (8.9%), NC (3.8%), SC (2.3%), SWC1 (1.1%), and SWC2 (0.8%). Consequently, the RX5D will be intensified over most regions of China under the 1.5 °C/2.0 °C warming targets, indicating the increased risk of flash floods in the future. In addition, RX5D will be even more severe under the 2.0 °C warming target.

To understand future changes in precipitation extremes under 1.5/2.0 °C warming targets more intuitively, Fig. 5 shows the percent changes in precipitation extremes averaged over China and its eight subregions. Clearly, most of the RCMs project more PRCPTOT under the 1.5 °C warming target (Fig. 5(a)). The results from the MME suggest a more than 5% increase over NEC, NC, CC, SWC2, NWC, and when

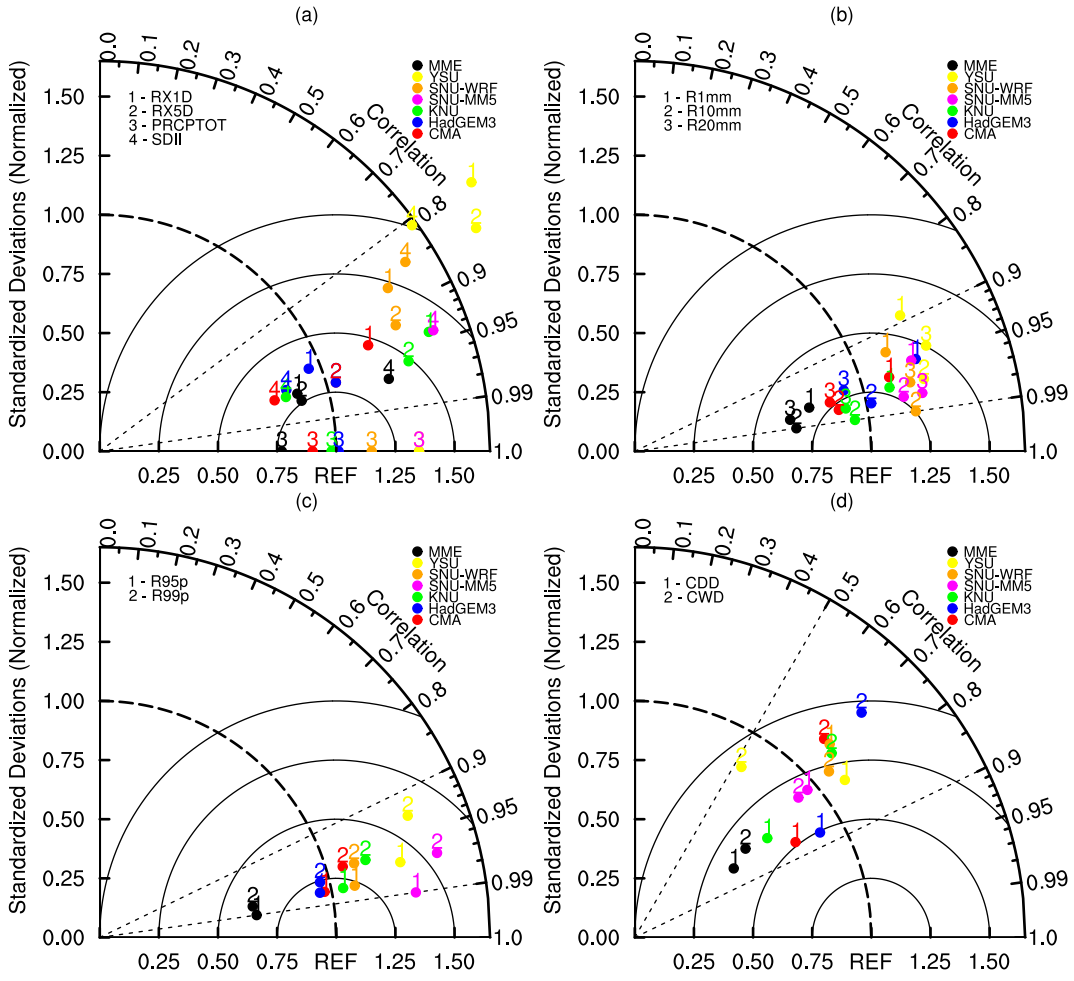

Fig. 2. Multivariable Taylor diagrams of the CMA (red), HadGEM3 (blue), KNU (green), SNU-MM5 (magenta), SNU-WRF (orange), YSU (yellow), and MME (black) simulated climatic means (1986–2005) by using eleven extreme precipitation indices in China. Each number represents an individual index.

considering China as a whole. In comparison with the MME, relatively weak increases are obtained from the CMA, with less than 5% for most of the regions. Under the 2.0 °C warming target, both the CMA and MME project an increase in PRCPTOT across China. Generally, increases over NEC, NC, EC, CC, SC, and NWC under the 1.5/2.0 °C warming targets are significant at the 90% confidence level (Fig. S3(a), (b)). With the additional 0.5 °C warming, most of the RCMs present an increase in PRCPTOT across China, especially over NWC (6.6%) and NC (6.7%), where the increases are significant at the 90% confidence level (Fig. S3 (c)). When considering China as a whole, PRCPTOT will increase by 1.4% via the CMA and 8.7% (6.7% to 11.2%) via the MME (model spread) at the 1.5 °C warming level, and it will continue to increase by 0.5% via the CMA and 1.9% (−0.6% to 4.1%) via the MME (model spread) due to the additional 0.5 °C warming.

Generally, changes in R95p (Fig. 5(b)) are much more similar to those in PRCPTOT (Fig. 5(a)). Most of the RCMs indicate that there will be an increase in R95p over China under the 1.5 °C warming target, with a more than 10% increase in the MME. In particular, increases over NWC, EC, CC, and SC are significant at the 90% confidence level (Fig. S3(b)). Under the 2.0 °C warming target, R95p will also increase across China, especially over NEC, NC, EC, CC, SC, and NWC, where the changes are significant at the 90% confidence level (Fig. S3(b)). Due to

Table 1
Climatological means of the eleven extreme precipitation indices during the historical period (1986–2005) based on CN05.1 and the RCMs from the CORDEX-East Asia project.

	CN05	CMA	HadGEM3	KNU	SNU-MM5	SNU-WRF	YSU	MME
CDD	56.3	45.1	52.8	38.8	52.7	57.6	60.7	52.0
CWD	11.5	12.9	14.6	12.3	10.4	11.6	9.2	11.8
PRCPTOT	560.4	557.7	558.9	546.6	580.3	577.5	570.6	564.6
R1mm	87.3	106.7	98.1	102.8	79.7	83.8	80.1	91.2
R10mm	14.9	12.3	14.4	13.0	15.6	16.9	16.4	14.8
R20mm	5.2	4.0	4.1	4.2	5.8	5.4	5.7	4.9
R95p	129.4	143.3	118.3	134.1	145.9	130.1	139.6	134.4
R99p	38.8	48.4	36.2	45.9	49.6	40.3	46.2	43.6
RX1D	34	34.9	28.6	34.3	45.3	36.9	42.8	36.7
RX5D	66.3	63.1	62.7	65.9	89.9	75.0	82.7	72.2
SDII	5.6	4.5	4.9	4.5	6.5	6.2	6.5	5.5

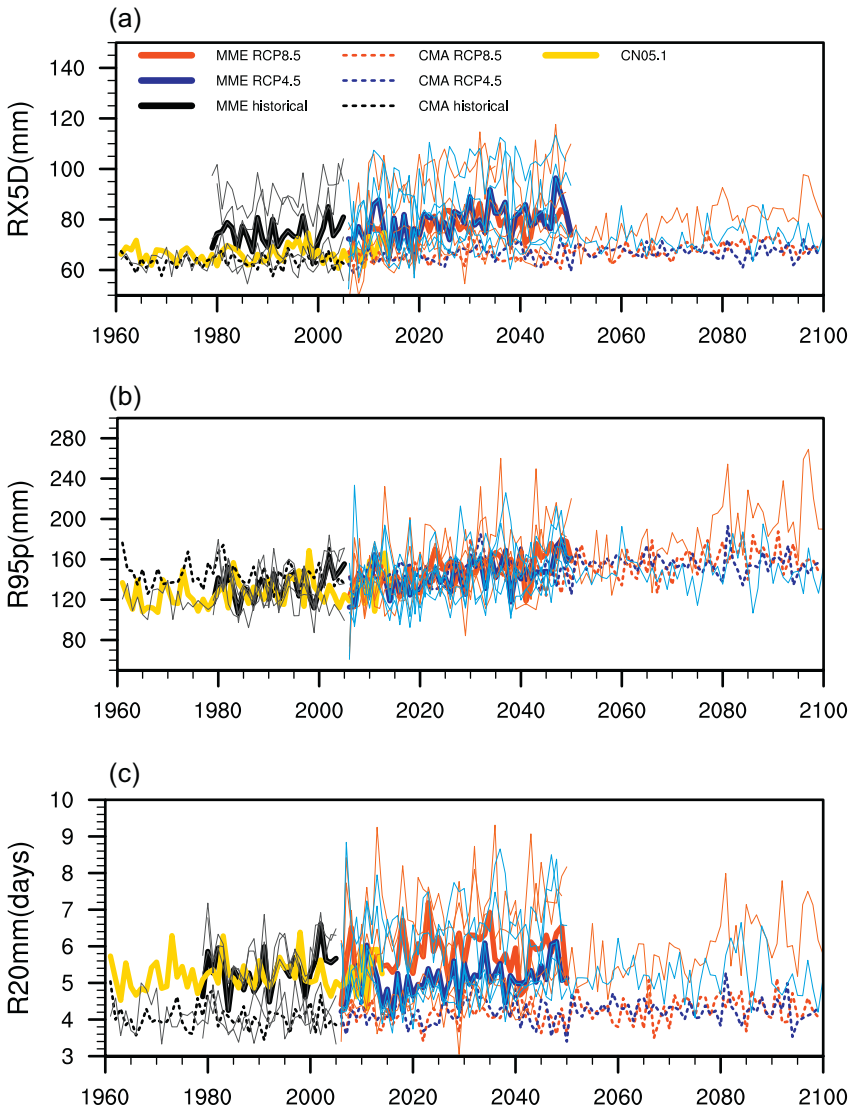

Fig. 3. Regional means of extreme precipitation indices in China calculated from CN05.1, the individual RCMs, and the MME for (a) RX5D (unit: mm), (b) R95p (unit: mm), and (c) R20mm (unit: days). The observation results based on CN05.1 from 1961 to 2014 are shown in yellow. The simulated historical series of the individual models from 1961 to 2005 are shown with black lines; the bold black line represents the historical ensemble median, and the dashed black line represents the historical CMA. Similarly, the colored lines show the projections from 2006 to 2100 (red for RCP8.5 and blue for RCP4.5).

the additional 0.5 °C warming, the R95p will further increase across China, and the increases over NWC (21.8%), NC (6.4%), and SWC1 (7.1%) are significant at the 90% confidence level. These changes will result in more severe precipitation extremes across China. When considering China as a whole, R95p is projected to increase under different warming targets, and it will further increase by 2.8% via the CMA and 3.6% (−2.2% to 8.6%) via the MME of the remaining RCMs (model spread) due to the additional 0.5 °C warming.

Unlike the other extreme precipitation indices, there is large uncertainty for changes in CDD over China and its eight subregions in the future (Fig. 5(c)). For the CMA, CDD is projected to decrease over NWC, NEC, NC, and SWC1, while it is projected to increase over EC, CC, SC, and SWC2. The changing signals are generally stronger under the 2.0 °C warming target when compared with the 1.5 °C warming target. For the MME, CDD is projected to increase over NEC, SC, and SWC1 under the 1.5 °C warming target, and they are significant at the 90% confidence level (Fig. S3(c)). However, CDD is projected to decrease over most regions of China under the 2.0 °C warming level. When considering China as a whole, CDD is projected to decrease via the CMA under the 1.5/2 °C warming targets, while large uncertainties can be seen from the other five RCMs, with model spreads ranging from −3.1% to 19.4% under the 1.5 °C warming target and − 8.4% to 18.3% under the 2.0 °C warming target. Despite the large uncertainty of future changes in CDD, all of the individual RCMs coincidently project a decrease in CDD across China due to the additional 0.5 °C of warming, especially over NEC (−10.5%), EC (−8.8%), and SWC2 (−6.2%), which are significant at the 90% confidence level. When considering China as a whole, CDD is projected to decrease by −1.7% via the CMA and − 5.1% (−5.3% to −1%) via the MME of the remaining RCMs (model spread) due to the additional 0.5 °C of warming.

Table 2 summarizes the percent changes of the eleven extreme precipitation indices averaged over China under the 1.5 °C/2.0 °C warming targets and the differences between these two warming targets. Accordingly, all of the indices (except for CDD) are projected to increase over China under different warming targets, which is consistent among the different RCMs. Furthermore, most of the individual RCMs predict that precipitation extremes will be further increased or strengthened with an additional 0.5 °C of warming. In particular, the nationally averaged R99p is projected to increase by 2.3% via the CMA and 19.9% via the MME under the 1.5 °C warming target. It will further increase by 5.5% via the CMA and 5.8% via the MME due to an additional 0.5 °C of warming. Similar results can also be found for R20mm (2.4% via the

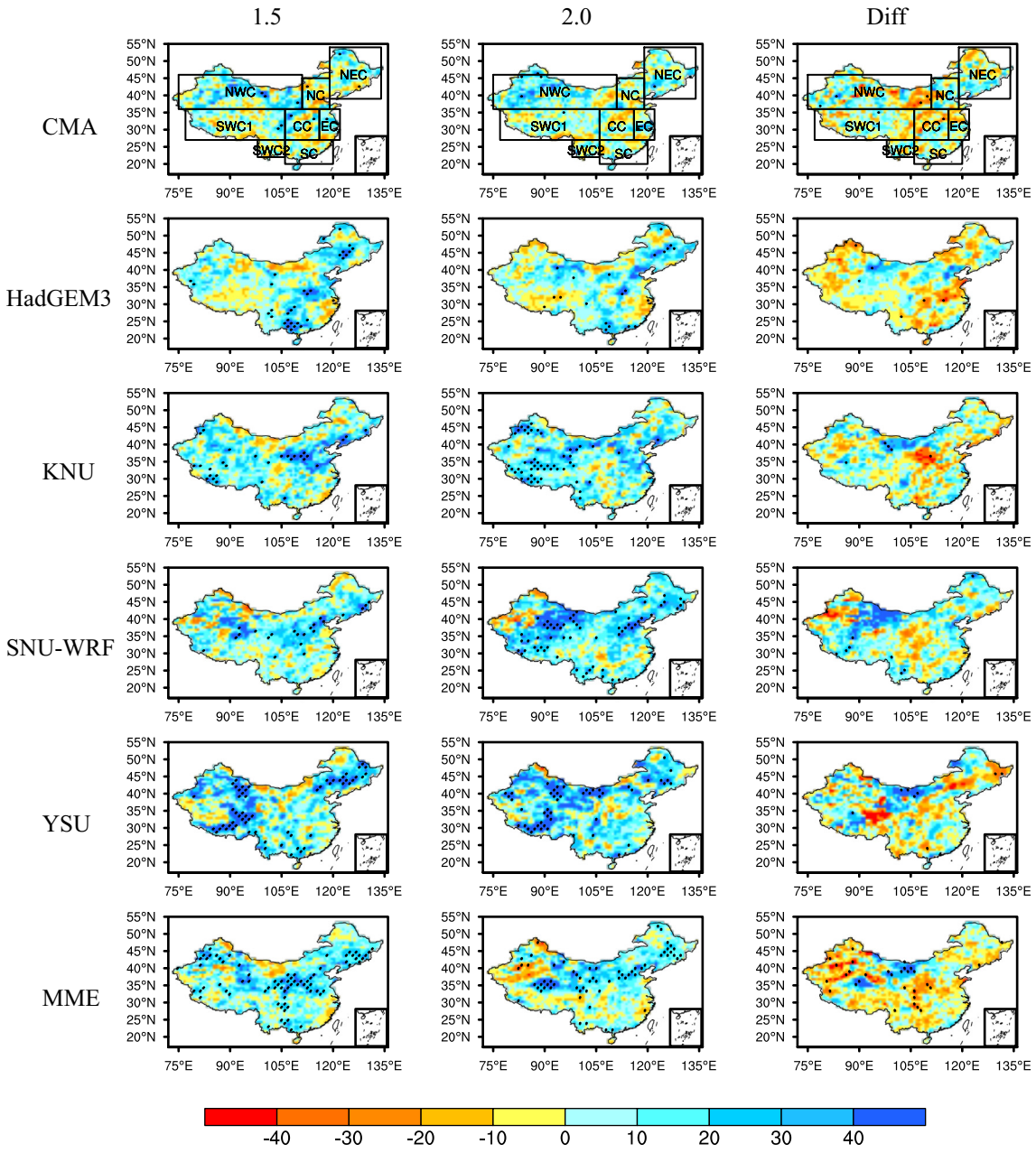

Fig. 4. Percent changes in RX5D across China for the 1.5 °C warming target (first column) and 2.0 °C warming target (middle column), in comparison with the historical mean (1986–2005), and the differences between the 2.0 °C and 1.5 °C warming (last column). The results are based on the RCP8.5 scenario. The black boxes identify the eight sub-regions analyzed in this study. The dotted regions represent the changes that are significant at the 90% confidence level based on the Student's *t*-test (unit: %).

CMA and 5.8% via the MME), R95p (2.8% via the CMA and 3.6% via the MME), RX1D (1.8% via the CMA and 1.3% via the MME), and RX5D (1.0% via both the CMA and MME) due to an additional 0.5 °C of warming. Therefore, the reoccurring risks of precipitation-related extreme events will evidently increase across China with additional warming in the future. The positive effects of limiting warming on changes in climate extremes are clear, and limiting warming should be encouraged regardless of the political and socioeconomic goals of a country.

To understand future changes in the recurrence of precipitation extremes over China, Fig. 6 further presents the probability density distribution and cumulative density distribution of RX1D and RX5D under the 1.5/2.0 °C warming targets. Since the trends for RX1D and RX5D during the historical period and different warming periods are not significant at 90% confidence level, we conduct an analysis based on the stationary GEV function in Eq. (4). The location parameters that are derived from the GEV distribution are 34.7 mm for RX1D and 67.2 mm for RX5D, which resemble the climatological means listed in Table 1. According to Fig. 6, the reoccurring probability of a damaging flood event will increase under these two warming targets. In particular, the 95% thresholds (corresponding to a 20-year event) of RX1D and RX5D during the historical period and two warming periods are analyzed. During the historical period, the threshold of a 20-year return event is 47.8 mm (97.6 mm) for RX1D (RX5D), and it will increase to 52.2 mm (105.9 mm) under the 1.5 °C warming target (blue lines) and 53.8 mm (108.3 mm) under the 2.0 °C warming target (red lines). Namely, the thresholds for the historical 20-year return event of RX1D (RX5D) will increase by 9.2% (8.5%) under the 1.5 °C warming target and 12.6% (11.0%) under the 2.0 °C warming target. A historical 20-year extreme precipitation event will become more likely to occur in the future; it will occur once every 8.8 years (11.5 years) for RX1D (RX5D) under the 1.5 °C warming target and every 6.9 years

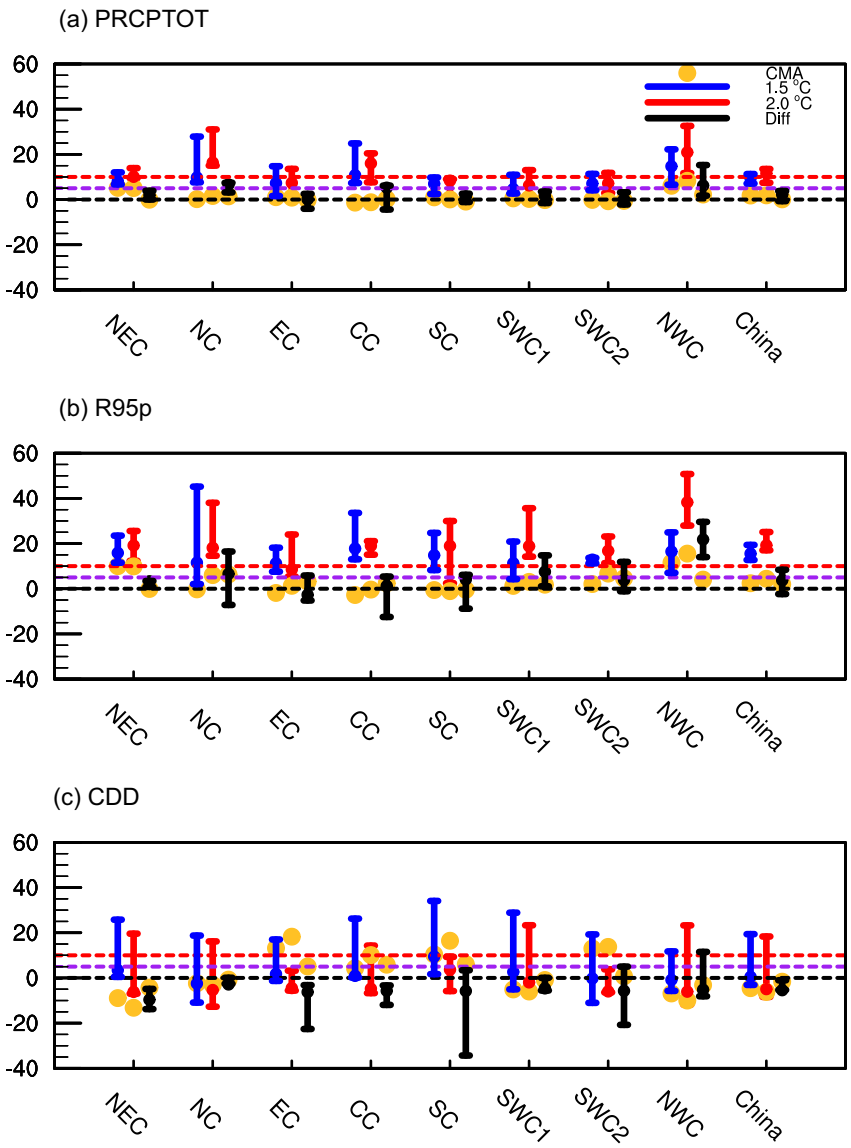

Fig. 5. Percent changes in (a) PRCPTOT, (b) R95p, and (c) CDD over China and its eight subregions under different warming targets (relative to the baseline of 1986–2005). The whiskers indicate the uncertainty ranges of the RCMs, and the dots represent the corresponding ensemble median (blue for 1.5 °C warming, red for 2.0 °C warming and black for their differences). The yellow dots represent the results from the CMA. The black horizontal dotted lines represent a 0% increase, the purple horizontal dotted lines represent a 5% increase, and the red horizontal dotted lines represent a 10% increase (unit: %).

(9.4 years) under the 2.0 °C warming target. Consequently, in the future, there will be a significant increase in the intensity and probability of 20-year return events for RX1D and RX5D, implying more flash floods across China. Therefore, limiting the additional 0.5 °C of warming is a good way to reduce the occurrence of flash floods in the future.

3.3. Changes in summer atmospheric circulations due to future warming

Extreme precipitation events over China mainly happen in summer, which is strongly affected by the East Asian summer monsoon (EASM) and other large-scale atmospheric systems (Ding et al., 2008). Therefore, we further investigate changes in summer atmospheric circulations under different warming targets. Generally, the geopotential heights at 500 hPa are projected to enhance significantly under the 1.5/2.0 °C warming targets (Fig. 7), especially over the northern regions (Fig. 7(a), (b)). In addition, the geopotential height will be further strengthened due to the additional 0.5 °C of warming (Fig. 7(c)). These warming patterns diminish the south-north temperature contrast, which results in weaker westerly winds within 20°N and 40°N at 200 hPa (Fig. S4(a), (b)). Anomalous easterly winds at 200 hPa help form an anticyclonic anomaly that is located between 15°N and 45°N (Fig. S4(a), (b)), which benefits divergence at upper levels over China. The increased contrast of SAT (figure not shown) and SLP (Fig. S4(d), (e)) between land and ocean will strengthen the EASM, which will bring more moisture into China from the Indian Ocean, South China Sea, and western North Pacific (Fig. 7(d), (e)). Then, increased water vapor transport (WVT) (Fig. 7(g), (h)) at low levels and an anticyclonic center at upper levels will provide a favorable environment for the increase in precipitation extremes over eastern China. In comparison with the 1.5 °C warming target, the anomalous anticyclonic center over northern China at 200 hPa (Fig. S4(c)) and the southeasterly wind anomalies at 850 hPa (Fig. 7(f)) will further strengthen under a 2.0 °C warming target. These anomalous circulations will help bring more water vapor (Fig. 7(i)) over China and provide a favorable environment for increased precipitation extremes over eastern China. All of the abovementioned analyses are significant at the 90% confidence level based on the Student's *t*-test and are similar to future changes based on GCMs (Chen et al., 2012b).

Table 2
Lists for the percent changes in the eleven extreme precipitation indices averaged over China under the 1.5/2 °C warming targets based on the CMA and MME compared with the baseline period of 1986–2005. The values inside the brackets indicate the ranges of the five RCMs that are initiated by the global climate model of HadGEM2-AO (unit: %).

	CMA			MME		
	1.5	2.0	Diff	1.5	2.0	Diff
CDD	−4.5	−6.2	−1.7	−0.3(−3.1,19.4)	−5.4(−8.4,18.3)	−5.1(−5.3,−1)
CWD	3.7	0.6	−3.0	6.5(2.7,12)	6.7(4.2,14.4)	0.2(−2.4,10.1)
PRCPTOT	1.4	1.9	0.5	8.7(6.7,11.2)	10.6(7.4,13.5)	1.9(−0.6,4.1)
R1mm	0.7	0.2	−0.5	2.7(0.3,3.3)	2.8(2.7,5.4)	0.1(0.2,2.4)
R10mm	1.3	2.0	0.6	11.5(8.9,13)	16.7(10.4,18.7)	5.2(1.5,6.1)
R20mm	2.3	4.7	2.4	19.1(19,22.4)	24.9(21.8,27.1)	5.8(−0.6,7.5)
R95p	1.6	4.4	2.8	14.0(12.2,19.1)	17.6(17.0,,25)	3.6(−2.2,8.6)
R99p	2.3	7.8	5.5	19.9(19.6,24.1)	25.7(18.8,36.9)	5.8(−5.3,15.1)
RX1D	4.2	6.1	1.8	10.0(8.1,16.2)	11.3(5.9,13.2)	1.3(−10.3,5.0)
RX5D	4.4	5.4	1.0	11.1(9.3,13.4)	12.1(6.0,13.5)	1.0(−7.4,4.2)
SDII	1.3	2.4	1.2	6.1(4.6,11)	7.5(5.2,10.1)	1.4(−0.9,2.8)

The variation in local convective precipitation generally presents a large contribution to extreme precipitation occurrences in the summer (Pendergrass et al., 2016). Thus, we also investigate future changes in summer convective precipitation over China (Fig. S4(g)–(i)). Clearly, convective precipitation will increase significantly over China under 1.5/2.0 °C warming targets, as both are significant at the 90% confidence level based on the Student's *t*-test. In addition, the percent changes in convective precipitation are greater than 40% over eastern China under the 1.5/2.0 °C warming targets, and they are also greater than 40% over northwestern China under the 2.0 °C warming target (Fig. S4 (g), (h)). Furthermore, changes in convective precipitation over China show many similarities to those in the extreme precipitation indices (e.g., R95p and PRCPTOT; Fig. S3). Due to the additional 0.5 °C warming, convective precipitation over China will further increase, and the increase over NWC is significant at the 90% confidence level (Fig. S4(i)).

4. Discussion and conclusion

Generally, future changes in precipitation vary among different regions around the world. For example, the eastern US is projected to become wetter in winter, while the northwest US and Great Plains are projected to become drier in summer under the 1.5/2.0 °C warming targets (Karmalkar and Bradley, 2017). Based on the CORDEX-Africa project, CDD over central Africa is projected to increase under the 1.5/2.0 °C warming targets (Mba et al., 2018). Due to the additional 0.5 °C of warming, CDD over central Africa is projected to further increase

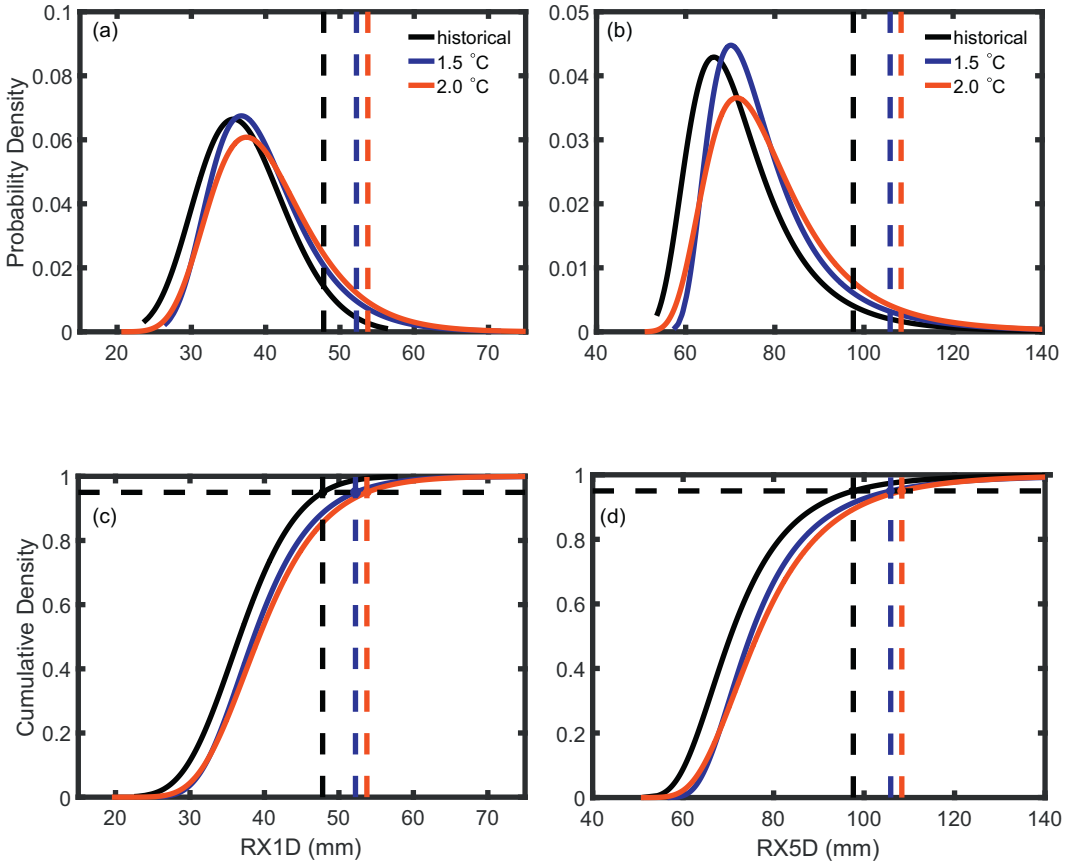

Fig. 6. Probability density distributions of (a) RX1D and (b) RX5D based on six RCMs. Cumulative density distributions of (c) RX1D and (d) RX5D based on six RCMs. The vertical dotted lines represent the thresholds of a 20-year return event. The black lines and curves represent the historical period of 1985–2006, the blue lines and curves represent the 1.5 °C warming, and the red lines and curves represent the 2.0 °C warming.

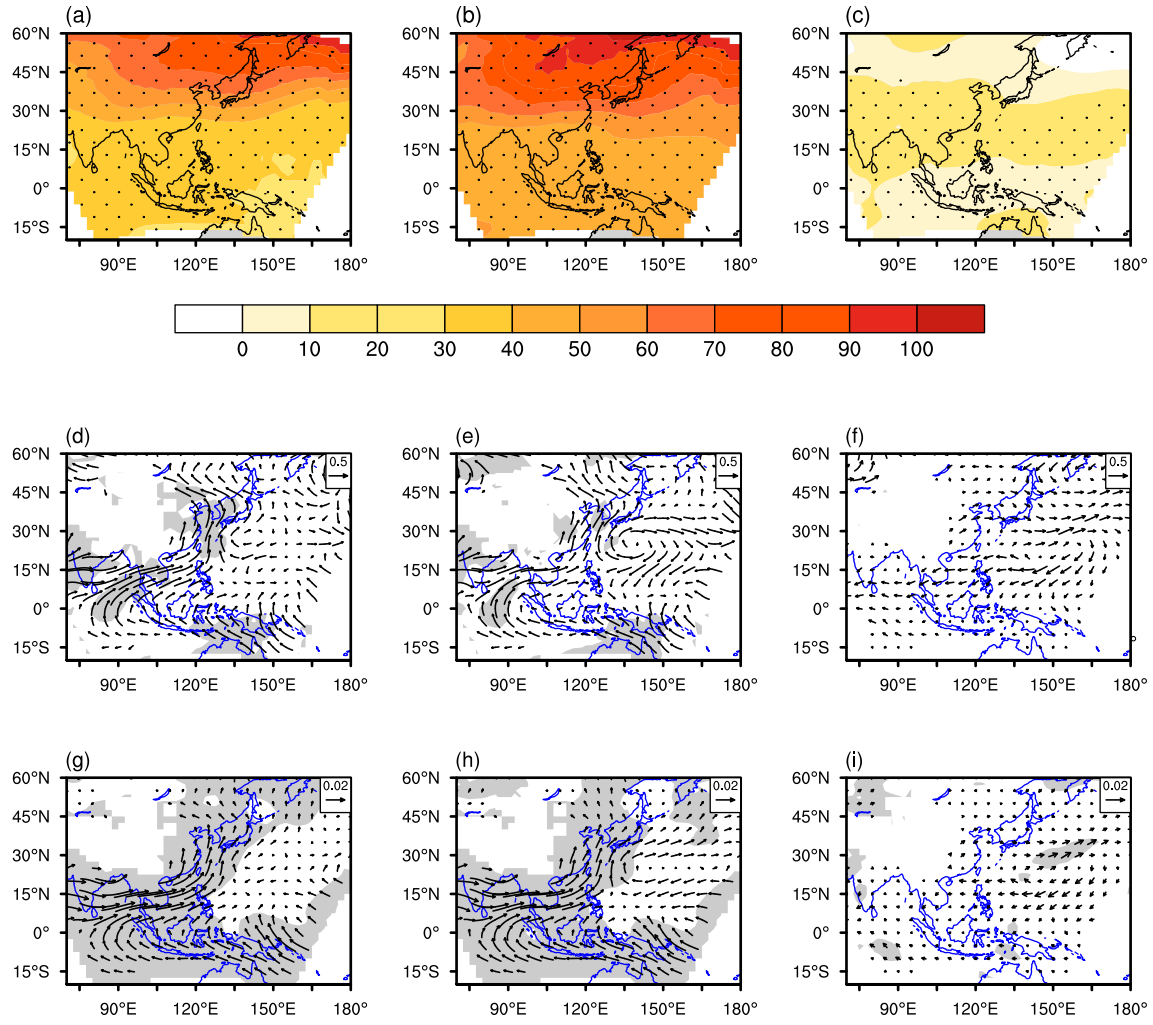

Fig. 7. Changes in future atmospheric circulations in summer under the 1.5 °C (first column) and 2.0 °C warming (middle column) targets with respect to the historical mean (1986–2005) and the differences between the 2.0 °C and 1.5 °C warming targets (last column). The upper row shows the 500 hPa geopotential height anomalies (unit: gpm), the middle row shows the 850 hPa wind anomalies (unit: m/s), and the bottom row shows the 850 hPa water vapor transport anomalies (unit: m/s). The dotted regions in (a)-(c) indicate the anomalies that are significant at the 99% confidence level based on the Student's *t*-test, and the shadings in (d)–(i) indicate the anomalies that are significant at the 90% confidence level based on the Student's *t*-test.

(Mba et al., 2018), which is contrary to that of China. Similar to central Africa, CDD over the Mediterranean region is projected to increase significantly due to the additional 0.5 °C of warming (Schleussner et al., 2016). In addition, changes in PRCPTOT over Africa also present different characteristics in comparison with those over China. Our study suggests that PRCPTOT will increase across China under the 1.5/2.0 °C warming targets, which is opposite of the change over the continent of Africa. However, Africa will be faced with more RX5D under the 1.5/2.0 °C warming targets (Wang et al., 2017; Mba et al., 2018), which is similar to that of China. Consistent with the increase in precipitation extremes over China, Wang et al. (2017) also indicated that precipitation extremes would increase worldwide due to the additional 0.5 °C of warming. In particular, RX5D is projected to increase in most regions under the 1.5 °C warming target, and significant increases can be found over eastern Russia, central Africa, and India due to the additional 0.5 °C of warming. Consequently, future changes in precipitation extremes have regional dependence, and the additional 0.5 °C of warming will cause increased effects worldwide.

In this study, RCM simulations of the CORDEX-East Asia project are implemented for the analysis of future changes in precipitation extremes over China under the 1.5/2.0 °C warming targets. All of the RCMs can reproduce the historical characteristics of precipitation extremes over China. In general, the MME outperforms the individual RCMs when simulating precipitation extremes over China. Under the 1.5/2.0 °C warming targets, the intensity, duration, and frequency of precipitation extremes will be more likely to increase across China. However, large uncertainties are identified for CDD over most sub-regions of China. According to the results of the MME, CDD is projected to increase significantly over SWC1, NEC, and SC under the 1.5 °C warming target, while it is generally projected to decrease across China under the 2.0 °C warming target. Due to the additional 0.5 °C of warming, precipitation extremes across China will be further strengthened; all of the RCMs suggest that flash floods are projected to be more severe over the eight sub-regions of China, while CDD is projected to decrease over China as a whole. In particular, the additional increase in total precipitation over NWC (6.6%) and NC (6.7%) and the additional increase in R95p over NWC (21.8%), NC (6.4%), and SWC1 (7.1%) are significant at the 90% confidence level. In terms of the nationally averaged extreme precipitation indices, the R20mm, R95p, R99p, RX1D, and RX5D values will increase by 2.3% (19.1%), 1.6% (14.0%), 2.3% (19.9%), 4.2% (10.0%), and 4.4% (11.1%) under the 1.5 °C warming target via the CMA (MME). These indices will further increase by 2.4% (5.8%), 2.8% (3.6%), 5.5% (5.8%), 1.8% (1.3%), and 1.0% (1.0%) respectively due to the additional 0.5 °C of warming. The results suggest that a stronger EASM and increased WVT might regulate increased precipitation extremes over eastern China, and increased local convective precipitation

might contribute to the significant increases in precipitation extremes over eastern China and northwestern China under the 1.5/2 °C warming targets. These changes in atmospheric circulation are even stronger due to the additional 0.5 °C of warming. Consequently, China will suffer from more frequent and severe extreme precipitation events with the increase in temperature in the future, and the probability for the occurrence of precipitation extremes will decrease when limiting the additional 0.5 °C of warming.

Acknowledgements

This research was jointly supported by the National Key Research and Development Program of China (Grant No: 2016YFA0600701), the External Cooperation Program of BIC, Chinese Academy of Sciences (Grant No: 134111KYSB20150016), the National Natural Science Foundation of China (Grant No: 41421004), and the CAS-PKU Joint Research Program.

Appendix A. Supplementary data

Supplementary data to this article can be found online at https://doi.org/10.1016/j.scitotenv.2018.05.324.

References

Aslam, A.Q., Ahmad, S.R., Ahmad, I., Hussain, Y., Hussain, M.S., 2017. Vulnerability and impact assessment of extreme climatic event: a case study of southern Punjab, Pakistan. Sci. Total Environ. 580:468–481. https://doi.org/10.1016/j.scitotenv.2016.11.155.

Cha, D.H., Lee, D.K., 2014. Reduction of systematic errors in regional climate simulations of the summer monsoon over East Asia and the western North Pacific by applying the spectral nudging technique. J. Geophys. Res. Atmos. 114:D14108. https://doi.org/10.1029/2008JD011176.

Chen, H.P., 2013. Projected change in extreme rainfall events in China by the end of the 21st century using CMIP5 models. Chin. Sci. Bull. 58:1462–1472. https://doi.org/10.1007/s11434-012-5612-2.

Chen, H.P., Sun, J.Q., 2014. Robustness of precipitation projections in China: comparison between CMIP5 and CMIP3 Models. Atmos. Ocean. Sci. Lett. 7:67–73. https://doi.org/10.3878/j.issn.1674-2834.13.0071.

Chen, H.P., Sun, J.Q., 2015. Assessing model performance of climate extremes in China: an intercomparison between CMIP5 and CMIP3. Clim. Chang. 129:197–211. https://doi.org/10.1007/s10584-014-1319-5.

Chen, H.P., Sun, J.Q., 2017. Contribution of human influence to increased daily precipitation extremes over China. Geophys. Res. Lett. 44:2435–2444. https://doi.org/10.1002/2016GL072439.

Chen, H.P., Sun, J.Q., 2018. Projected changes in climate extremes in China in a 1.5°C warmer world. Int. J. Climatol. https://doi.org/10.1002/joc.5221.

Chen, H.P., Sun, J.Q., Fan, K., 2012a. Decadal features of heavy rainfall events in eastern China. Acta Meteorol. Sin. 26:289–303. https://doi.org/10.1007/s13351-012-0303-0.

Chen, H.P., Sun, J.Q., Chen, X.L., 2012b. The projection and uncertainty analysis of summer precipitation in China and the variations of associated atmospheric circulation field. Clim. Environ. Res. 17 (2), 171–181 (in Chinese).

Chen, H.P., Sun, J.Q., Chen, X.L., 2013. Future changes of drought and flood events in China under a global warming scenario. Atmos. Ocean. Sci. Lett. 6, 8–13.

Chen, H.P., Sun, J.Q., Li, H.X., 2017. Future changes in precipitation extremes over China using the NEX-GDDP high-resolution daily downscaled data-set. Atmos. Ocean. Sci. Lett. (6), 403–410.

Cheng, J., Wu, J.J., Xu, Z.W., Zhu, R., Wang, X., Li, K.S., Wen, L.Y., Yang, H.H., Su, H., 2014. Associations between extreme precipitation and childhood hand, foot and mouth disease in urban and rural areas in Hefei, China. Sci. Total Environ. 497-498:484–490. https://doi.org/10.1016/j.scitotenv.2014.08.006.

Davies, T., Cullen, M.J.P., Malcolm, A.J., Mawson, M.H., Staniforth, A., White, A.A., Wood, N., 2005. A new dynamical core for the Met Office's global and regional modeling of the atmosphere. Q. J. R. Meteorol. Soc. 131:1759–1782. https://doi.org/10.1256/qj.04.101.

Ding, Y.H., Wang, Z.Y., Sun, Y., 2008. Inter-decadal variation of the summer precipitation in East China and its association with decreasing Asian summer monsoon. Part I: observed evidences. Int. J. Climatol. 28 (9):1139–1161. https://doi.org/10.1002/joc.1615.

Dong, S.Y., Xu, Y., Zhou, B.T., Shi, Y., 2015. Assessment of indices of temperature extremes simulated by multiple CMIP5 models over China. Adv. Atmos. Sci. 32 (8):1077–1091. https://doi.org/10.1007/s00376-015-4152-5.

Gao, X.J., Shi, Y., Giorgi, F., 2016. Comparison of convective parameterizations in RegCM4 experiments over China with CLM as the land surface model. Atmos. Ocean. Sci. Lett. 9:246–254. https://doi.org/10.1080/16742834.2016.1172938.

Giorgi, F., Gao, X.J., 2018. Regional earth system modeling: review and future directions. Atmos. Ocean. Sci. Lett. 8:1–9. https://doi.org/10.1080/16742834.2018.1452520.

Giorgi, F., Coppola, E., Solmon, F., Mariotti, L., Sylla, M., Bi, X., Elguindi, N., Diro, G., et al., 2012. RegCM4: model description and preliminary tests over multiple CORDEX domains. Clim. Res. 52:7–29. https://doi.org/10.3354/cr01018.

Gleckler, P.J., Taylor, K.E., Doutriaux, C., 2008. Performance metrics for climate models. J. Geophys. Res. Atmos. 113:304–312. https://doi.org/10.1029/2007JD008972.

Guo, X.J., Huang, J.B., Luo, Y., Zhao, Z.C., Xu, Y., 2016. Projection of precipitation extremes for eight global warming targets by 17 CMIP5 models. Nat. Hazards 84:2299–2319. https://doi.org/10.1007/s11069-016-2553-0.

Hong, S.Y., Park, H., Cheong, H.B., Kim, J.E.E., Koo, M.S., Jang, J., Ham, S., Hwang, S.O., et al., 2013. The global/regional integrated model system (GRIMs). Asia-Pac. J. Atmos. Sci. 49 (2):219–243. https://doi.org/10.1007/s13143-013-0023-0.

Huang, J.P., Yu, H.P., Dai, A.G., Wei, Y., Kang, L.T., 2017. Drylands face potential threat under 2 °C global warming target. Nat. Clim. Chang. 7:417–422. https://doi.org/10.1038/nclimate3275.

IPCC, 2013. Climate Change 2013: The Physical Science Basis. Contribution of Working Group I to the Fifth Assessment Report of the Intergovernmental Panel on Climate Change. Cambridge University Press, Cambridge, UK, and New York, NY (1535pp).

Jin, C.S., Cha, D.H., Lee, D.K., Suh, M.S., Hong, S.Y., Kang, H.S., Ho, C.H., 2015. Evaluation of climatological tropical cyclone activity over the western North Pacific in the CORDEX-East Asia multi-RCM simulations. Clim. Dyn. 47 (1–14). https://doi.org/10.1007/s00382-015-2869-6.

Karmalkar, A.V., Bradley, R.S., 2017. Consequences of global warming of 1.5 °C and 2 °C for regional temperature and precipitation changes in the contiguous United States. PLoS One 12, e0168697. https://doi.org/10.1371/journal.pone.0168697.

Kim, J., Waliser, D.E., Mattmann, C.A., Goodale, C.E., Hart, A.F., Zimdars, P.A., Crichton, D.J., Jones, C., et al., 2014. Evaluation of the CORDEX-Africa multi-RCM hindcast: systematic model errors. Clim. Dyn. 42:1189–1202. https://doi.org/10.1007/s00382-013-1751-7.

Kim, Y., Jun, M., Min, S.K., Suh, M.S., Kang, H.S., 2016. Spatial analysis of future East Asian seasonal temperature using two regional climate model simulations. Asia-Pac. J. Atmos. Sci. 52 (2):237–249. https://doi.org/10.1007/s13143-016-0022-z.

King, A.D., Karoly, D.J., Henley, B.J., 2017. Australian climate extremes at 1.5 °C and 2 °C of global warming. Nat. Clim. Chang. 7:412–416. https://doi.org/10.1038/nclimate3296.

Li, J.F., Zhang, Q., Chen, Y.Q., Singh, V.P., 2015. Future joint probability behaviors of precipitation extremes across China: spatiotemporal patterns and implications for flood and drought hazards. Glob. Planet. Chang. 124:107–122. https://doi.org/10.1016/j.gloplacha.2014.11.012.

Li, H.X., Chen, H.P., Wang, H.J., 2017. Effects of anthropogenic activity emerging as intensified extreme precipitation over China. J. Geophys. Res. Atmos. 122:6899–6914. https://doi.org/10.1002/2016JD026251.

Liu, R., Chen, L.S., Cicerone, R.J., Chein-Jung, S., Jun, L.I., Wang, J., Zhang, Y., 2015. Trends of extreme precipitation in eastern China and their possible causes. Adv. Atmos. Sci. 32:1027–1037. https://doi.org/10.1007/s00376-015-5002-1.

Liu, A., Soneja, S.I., Jiang, C.S., Huang, C.J., Kerns, T., Beck, K., Mitchell, C., Sapkota, A., 2017a. Frequency of extreme weather events and increased risk of motor vehicle collision in Maryland. Sci. Total Environ. 580:550–555. https://doi.org/10.1016/j.scitotenv.2016.11.211.

Liu, J., Du, H.B., Wu, Z.F., Hong, H.S., Wang, L., Zong, S.W., 2017b. Recent and future changes in the combination of annual temperature and precipitation throughout China. Int. J. Climatol. 37 (2):821–833. https://doi.org/10.1002/joc.4742.

Martins, E.S., Stedinger, J.R., 2000. Generalized maximum-likelihood generalized extreme-value quantile estimators for hydrologic data. Water Resour. Res. 36:737–744. https://doi.org/10.1029/1999WR900330.

Mba, W.P., Longandjo, G.N., Moufouma-Okia, W., Bell, J.P., James, R., Haensler, A., Nguemo, T.C.F., Guenang, G.M., Tchotochou, A.L.D., 2018. Consequences of 1.5 °C and 2 °C global warming levels for temperature and precipitation changes over Central Africa. Environ. Res. Lett. 13, 055011.

Oh, S.G., Suh, M.S., Cha, D.H., 2013. Impact of lateral boundary conditions on precipitation and temperature extremes over South Korea in the CORDEX regional climate simulation using RegCM4. Asia-Pac. J. Atmos. Sci. 49:497–509. https://doi.org/10.1007/s13143-013-0044-8.

Oh, S.G., Park, J.H., Lee, S.H., Suh, M.S., 2014. Assessment of the RegCM4 over East Asia and future precipitation change adapted to the RCP scenarios. J. Geophys. Res. Atmos. 119 (6):2913–2927. https://doi.org/10.1002/2013JD020693.

Ozturk, T., Altinsoy, H., Turkes, M., Kurnaz, L.M., 2012. Simulation of temperature and precipitation climatology for the Central Asia CORDEX domain using RegCM 4.0. Clim. Res. 52:63–76. https://doi.org/10.3354/cr01082.

Park, C., Min, S.K., Lee, D., Cha, D.H., Suh, M.S., Kang, H.S., Hong, S.Y., Lee, D.K., et al., 2016. Evaluation of multiple regional climate models for summer climate extremes over East Asia. Clim. Dyn. 46 (1–18).

Pendergrass, A.G., Reed, K.A., Medeiros, B., 2016. The link between extreme precipitation and convective organization in a warming climate: global radiative-convective equilibrium simulations. Geophys. Res. Lett. https://doi.org/10.1002/2016GL071285.

Piras, M., Mascaro, G., Deidda, R., Vivoni, E.R., 2016. Impacts of climate change on precipitation and discharge extremes through the use of statistical downscaling approaches in a Mediterranean basin. Sci. Total Environ. 543:952–964. https://doi.org/10.1016/j.scitotenv.2015.06.088.

Qian, W.H., Lin, X., 2005. Regional trends in recent precipitation indices in China. Meteorog. Atmos. Phys. 90 (3–4):193–207. https://doi.org/10.1007/s00703-004-0101-z.

Schleussner, C.F., Lissner, T.K., Fischer, E.M., Wohland, J., Perrette, M., Golly, A., Rogelj, J., Childers, K., et al., 2016. Differential climate impacts for policy-relevant limits to global warming: the case of 1.5 °C and 2 °C. Earth Syst. Dynam. 7:327–351. https://doi.org/10.5194/esd-7-327-2016.

Skamarock, W.C., Klemp, J.B., Dudhia, J., Gill, D.O., Barker, D.M., Wang, W., Powers, J.G., 2005. A description of the advanced research WRF version 2. NCAR Technical 113:7–25. https://doi.org/10.5065/D68S4MVH.

Sperna Weiland, F.C., van Beek, L.P.H., Kwadijk, J.C.J., Bierkens, M.F.P., 2010. The ability of a GCM-forced hydrological model to reproduce global discharge variability. Hydrol. Earth Syst. Sci. 14:1595–1621. https://doi.org/10.5194/hess-14-1595-2010.

Sun, J.Q., Ao, J., 2013. Changes in precipitation and extreme precipitation in a warming environment in China. Sci. Bull. 58:1395–1401. https://doi.org/10.1007/s11434-012-5542-z.

Tian, D., Guo, Y., Dong, W.J., 2015. Future changes and uncertainties in temperature and precipitation over China based on CMIP5 models. Adv. Atmos. Sci. 32 (4):487–496. https://doi.org/10.1007/s00376-014-4102-7.

Tian, D., Dong, W.J., Zhang, H., Guo, Y., Yang, S.L., Dai, T.L., 2017. Future changes in coverage of 1.5 °C and 2 °C warming thresholds. Sci. Bull. 62 (21):1445–1463. https://doi.org/10.1016/j.scib.2017.09.023.

UNFCCC, 2015. Adoption of the Paris Agreement. Preprints. United Nations Office at Geneva, Switzerland (FCCC/CP/2015/L.2019/Rev.2011).

Wang, L., Chen, W., 2014. A CMIP5 multimodel projection of future temperature, precipitation, and climatological drought in China. Int. J. Climatol. 34:2059–2078. https://doi.org/10.1002/joc.3822.

Wang, H.J., Sun, J.Q., Chen, H.P., Zhu, Y.L., Zhang, Y., Jiang, D.B., Lang, X.M., Fan, K., et al., 2012. Extreme climate in China: facts, simulation and projection. Meteorol. Z. 21: 279–304. https://doi.org/10.1127/0941-2948/2012/0330.

Wang, Z.L., Lin, L., Zhang, X.Y., Zhang, H., Liu, L.K., Xu, Y.Y., 2017. Scenario dependence of future changes in climate extremes under 1.5 °C and 2 °C global warming. Sci. Rep. 7, 46432. https://doi.org/10.1038/srep46432.

Wilks, D.S., 2011. Statistical Methods in the Atmospheric Sciences. Academic Press, The Boulevard, Langford Lane, Kidlington, Oxford, U. K., pp. 105–109.

World Meteorological Organization Current Extreme Weather Events (WMO), 2010. www.wmo.int/pages/mediacentre/news/extremeweathersequence_en.html.

Wu, J., Gao, X.J., 2013. A gridded daily observation dataset over China region and comparison with the other datasets. Chin. J. Geophys. 56:1102–1111 (in Chinese). https://doi.org/10.6038/cjg20130406.

Wu, J., Zhou, B.T., Xu, Y., 2016. Response of precipitation and its extremes over China to warming: CMIP5 simulation and projection. Chin. J. Geophys. 58 (9):3048–3060. https://doi.org/10.6038/cjg20150903.

Xu, Y., Gao, X.J., Yan, S., Chonghai, X.U., Ying, S., Giorgi, F., 2009. A daily temperature dataset over China and its application in validating a RCM simulation. Adv. Atmos. Sci. 26:763–772. https://doi.org/10.1007/s00376-009-9029-z.

Xu, Y., Wu, J., Shi, Y., Zhou, B.T., Li, R.K., Wu, J., 2015a. Change in extreme climate events over China based on CMIP5. Atmos. Ocean. Sci. Lett. 8 (4), 185–192.

Xu, Y., Gao, X.J., Shi, Y., Zhou, B.T., 2015b. Detection and attribution analysis of annual mean temperature changes in China. Clim. Res. 63:61–71. https://doi.org/10.3354/cr01283.

Xu, Y., Zhou, B.T., Wu, J., Han, Z.Y., Zhang, Y.X., Wu, J., 2017. Asian climate change under 1.5–4 °C warming targets. Adv. Clim. Chang. Res. (2):99–107 https://doi.org/10.1016/j.accre.2017.05.004.

Ye, J.S., Pei, J.Y., Fang, C., 2018. Under which climate and soil conditions the plant productivity–precipitation relationship is linear or nonlinear? Sci. Total Environ. 616-617:1174–1180. https://doi.org/10.1016/j.scitotenv.2017.10.203.

Zhai, P.M., Zhang, X.B., Wan, H., Pan, X.H., 2005. Trends in Total precipitation and frequency of daily precipitation extremes over China. J. Clim. 18:1096–1108. https://doi.org/10.1175/JCLI-3318.1.

Zhou, B.T., Xu, Y., Wu, J., Dong, S.Y., Shi, Y., 2015. Changes in temperature and precipitation extreme indices over China: analysis of a high-resolution grid dataset. Int. J. Climatol. 36 (3):1051–1066. https://doi.org/10.1002/joc.440.

Zhou, T.J., Sun, N., Zhang, W.X., Chen, X.L., Peng, D.D., Li, D.H., Ren, L.W., Zuo, M., 2018. When and how will the millennium silk road witness 1.5 °C and 2 °C warmer worlds? Atmos. Ocean. Sci. Lett. 11 (2), 180–188.